JOURNAL OF ADVANCED TRANSPORTATION
J. Adv. Transp. 2015; **49**:434–456
Published online 18 July 2014 in Wiley Online Library (wileyonlinelibrary.com). DOI: 10.1002/atr.1281

Constrained H_∞ control of urban transportation network

Huide Zhou*, Rachid Bouyekhf and Adbellah EL Moudni

Laboratoire Systèmes et Transports (SeT), Université de Technologie de Belfort-Montbéliard (UTBM), Rue Thierry Mieg, 90010 Belfort Cedex, France

SUMMARY

Because transportation systems involve massive complex human activities, there exist substantial unpredictable uncertainties of the traffic demands. This paper aims at presenting an H_∞ control method for transportation network that can enhance the tolerance of the system due to these uncertainties. In particular, the store-and-forward approach is applied to model the system into a linear form. Then, a detailed controllability analysis shows that the system is not completely controllable by taking the constraints on the green times into account. This makes difficult to apply directly the H_∞ method. To overcome this difficulty, this paper isolates the fully controllable part of the transportation system, and the problem of disturbance attenuation is then solved by means of a convex optimization with linear matrix inequality. Finally, the simulation of a large-scale hypothetical network is carried out to illustrate the results. Copyright © 2014 John Wiley & Sons, Ltd.

KEY WORDS: urban transportation network; controllability; constrained H_∞ control; LMI

1. INTRODUCTION

Urban transportation is an essential part of the modern cities. Because of the rapid increase of traffic demands in recent decades, the congestion problem emerges more frequently, which leads to serious economic and environment issues. This situation has encouraged the researchers to develop advanced traffic signal control strategies.

The conventional strategies optimized the signal timing schedules off-line by using historical data, which are also called fixed-time strategies. For example, TRANSYT is a well-known off-line computer program for modeling transportation systems and designing traffic signal schedules, which was first presented by the Transport Research Laboratory [1]. However, fixed-time strategies do not concern the real-time data of traffic demands, which makes them not capable to fit current serious deterioration of urban transportation. To improve this situation, traffic-responsive strategies have been developed to take the dynamic of traffic demands into account. One of the most known works is the split, cycle, and offset optimization technique (SCOOT) [2], which applies the TRANSYT model fed by the real-time data and searches the beneficial incremental regulations of signal schedules. The major drawback of SCOOT is the bad performances in case of saturated traffic conditions [3]. Another notable approach is the application of the kinetic wave theory and its first-order approximation: cell transmission model (CTM) [4]. Because CTM shows very high accuracy [5], it has been widely applied in traffic engineering (e.g., [6]). However, the accuracy is based on the complexity of the model, which makes it difficult to design efficient real-time controllers. Recently, an interesting work, called the traffic-responsive urban control strategy, has been presented, which was developed for the European Telematics Applications in Transport project TABASCO [7]. This strategy applies the store-and-forward model, which was initially developed in [8]. Such model has a linear form; hence, it opens the way to apply highly efficient control methods with polynomial complexity, which, on its turn, allows real-time signal control for the

*Correspondence to: Huide Zhou, Laboratoire Systèmes et Transports (SeT), Université de Technologie de Belfort-Montbéliard (UTBM), Rue Thierry Mieg, 90010 Belfort Cedex, France. E-mail: huide.zhou@utbm.fr

transportation networks, even with a large scale. This is a huge advantage, and consequently, such model has been also applied in many other control strategies in the recent decade (e.g., [9–11]).

Note that most of the aforementioned strategies were developed with demand analysis in some nominally "typical" conditions. However, because the urban transportation involves massive random human activities, the uncertainties in traffic demands substantially exist and have considerable consequences for the behaviors of the system [12]. Hence, the robustness due to these uncertainties should be concerned by traffic signals. There have been many researches that take this problem into account. First, certain optimizations on fixed-time signal plans have been addressed (e.g., [13–16]). For the traffic-responsive control, a notable work was presented in [17], which captures the uncertainties in origin–destination demands and develops a robust control method on the basis of CTM. However, because of the complexity of CTM, such method works only for single intersections. Most recently, the rolling-horizon control paradigm has also been applied in this field. For example, Tettamanti *et al.* [18, 19] proposed a robust model predictive control strategy by using the store-and-forward model. Another interesting work presented in [20] formulated the problem into a mixed-integer linear programming problem based on the S model. In our opinion, such paradigm suffers from the large computational demand in real time, which increases the cost of the strategy and hence may limit its application.

In this context, this paper endeavors to elaborate an efficient traffic-responsive signal split control strategy that can enhance the robustness due to the uncertainties in traffic demands. For this purpose, we choose the store-and-forward linear model and apply H_∞ control method in the transportation context. A major difference with the existing works is the controllability analysis of the system, which indicates that the transportation network is not completely controllable by the green time split. As a result, the decomposition is imposed to isolate the controllable part of the system. By focusing on this subsystem, a constrained H_∞ control problem is formulated to maximize the tolerance of system due to the uncertainties in traffic demands. The solution is then presented by combining traditional H_∞ control method with some additional linear conditions.

This paper is organized as follows. Section 2 presents the urban transportation network model. The controllability of this model is analyzed in Section 3, and the decomposition is performed to isolate the completely controllable subsystem. Then, Section 4 is devoted in the H_∞ control method to present an optimal traffic signal control strategy. Finally, Section 5 considers a large-scale hypothetical network as an example to illustrate and compare our results with the work of Diakaki *et al.* [7].

2. TRANSPORTATION NETWORK MODELING

The store-and-forward based approach is a widely applied macroscopic transportation modeling concept [3, 8]. Indeed, considering the lane i in a transportation network including n traffic lanes (Figure 1), the dynamics of its number of vehicles x_i is given by

$$x_i(k+1) = x_i(k) + T\left[r_i(k) - d_i(k) + \sum_{j=1,j\neq i}^{n} \sigma_{i,j}(k) - \sum_{j=1,j\neq i}^{n} \sigma_{j,i}(k)\right] \tag{1}$$

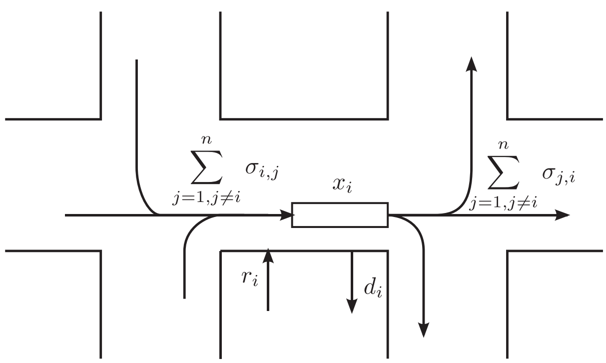

Figure 1. The flows related with the lane i.

DOI: 10.1002/atr

It is important to note that only the terms corresponding to actual links between lanes of the network are made explicit in Equation (1). Otherwise, all the $\sigma_{i,j}$ for non-existing links do not appear in the equations.

The basic idea of the store-and-forward model is to consider the total outflow rate of any lane during a step as its average value (Figure 2), which leads to $\forall\, i \in \{1, \cdots, n\}$ [8]

$$\sum_{j=1, j\neq i}^{n} \sigma_{j,i} = \frac{g_i s_i}{c} \tag{2}$$

Hence, by using the turning rates $\lambda_{i,j} \in [0, 1]$, the inflow rates are given by

$$\sigma_{i,j} = \lambda_{i,j} \frac{g_j s_j}{c} \tag{3}$$

It is obvious that the exit flow is a part of the total inflow; hence, we have

$$d_i = \lambda_{i,i} \sum_{j=1, j\neq i}^{n} \sigma_{i,j} = \lambda_{i,i} \sum_{j=1, j\neq i}^{n} \lambda_{i,j} \frac{g_j s_j}{c} \tag{4}$$

Note that this approach models the system into a linear form and hence significantly simplifies the problem. It is inevitable that such simplification also leads to a few consequences as follows:

(1) The step T cannot be shorter than the cycle time c; hence, the oscillations of vehicle numbers due to the green/red commutations cannot be described by the model [3].
(2) Equation (2) implies that the outflows of all lanes are considered saturated; the under-saturated and over-saturated (spill-back) situations are not concerned by the model.
(3) Equations (3) and (4) imply that the turning rates and the exit rates are predetermined; hence, the model cannot consider the uncertainties of these parameters.

Now, by replacing Equations (2), (3) and (4) in Equation (1) and by combining all lanes, the transportation network with any arbitrary size, topology and characteristics can be modeled into the following linear state-space difference equation

$$x(k+1) = x(k) + Lg(k) + Tr(k) \tag{5}$$

where $x = [x_1, \cdots, x_n]^T$, $g = [g_1, \cdots, g_n]^T$, $r = [r_1, \cdots, r_n]^T$, and the matrix L is determined by the saturation flow rates, turning rates and exit rates according to Equations (2), (3) and (4). More details of this store-and-forward modeling are seen in [7, 21].

However, this model does not consider the relationships between the green times. In the following, we will show that the green times $g_1, \cdots, g_n$ are not independent variables. To do this, consider first an intersection with two phases (Figure 3). Let g_{e1} and g_{e2} denote effective green times of two phases, and let g_1, g_2, g_3 and g_4 be the green times corresponding to four entry lanes. It is clear that

$$g_1 = g_2 = g_{e1}, \quad g_3 = g_4 = g_{e2} \tag{6}$$

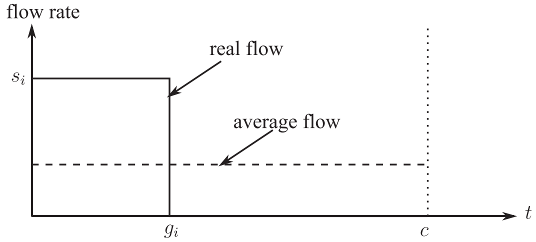

Figure 2. Simplification of store-and-forward approach.

DOI: 10.1002/atr

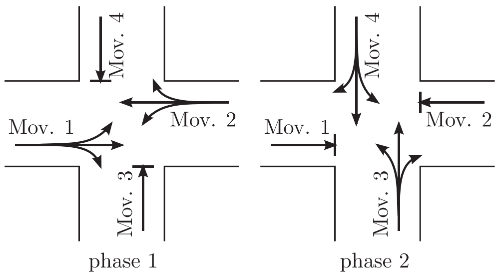

Figure 3. Two-phase intersection.

Note that g_{e1} and g_{e2} always satisfy the following relationship:

$$g_{e1} + g_{e2} = c - \chi \tag{7}$$

where χ is the total lost time of this intersection in one cycle. Generally, the lost times and the cycle are considered fixed and known [7]. Consequently, there is only one independent variable in this intersection. If g_{e1} is chosen as the control variable, the green times of all lanes can be represented by the following linear relationship:

$$\begin{pmatrix} g_1 \\ g_2 \\ g_3 \\ g_4 \end{pmatrix} = \begin{pmatrix} g_{e1} \\ g_{e1} \\ g_{e2} \\ g_{e2} \end{pmatrix} = \begin{pmatrix} 1 \\ 1 \\ -1 \\ -1 \end{pmatrix} g_{e1} + \begin{pmatrix} 0 \\ 0 \\ c-\chi \\ c-\chi \end{pmatrix} \tag{8}$$

Consider another example illustrated in Figure 4. This intersection involves six movements, and its cycle is divided into three phases. Let g_{e1}, g_{e2} and g_{e3} be the effective green times of three phases, and let g_i be the green time of the lane $i = 1, \cdots, 6$. In this case, certain lanes correspond to more than one phase (e.g., lane 2 is approved in both phases 1 and 2). More precisely, we have the following relationship:

$$\begin{pmatrix} g_1 \\ g_2 \\ g_3 \\ g_4 \\ g_5 \\ g_6 \end{pmatrix} = \begin{pmatrix} g_{e1} \\ g_{e1} + g_{e3} \\ g_{e3} \\ g_{e2} + g_{e3} \\ g_{e2} \\ g_{e1} + g_{e2} \end{pmatrix} \tag{9}$$

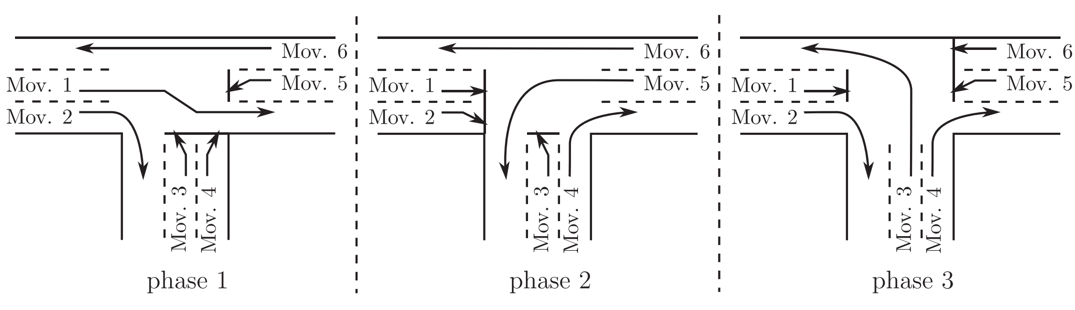

Figure 4. Three phases of T-intersection.

DOI: 10.1002/atr

Furthermore, similar with the two-phase case, we have in this intersection

$$g_{e1} + g_{e2} + g_{e3} = c - \chi \tag{10}$$

which indicates that there are two independent control variables. Thus, if g_{e1} and g_{e2} are chosen as control variables, it follows

$$\begin{pmatrix} g_1 \\ g_2 \\ g_3 \\ g_4 \\ g_5 \\ g_6 \end{pmatrix} = \begin{pmatrix} 1 & 0 \\ 0 & -1 \\ -1 & -1 \\ -1 & 0 \\ 0 & 1 \\ 1 & 1 \end{pmatrix} \begin{pmatrix} g_{e1} \\ g_{e2} \end{pmatrix} + \begin{pmatrix} 0 \\ c-\chi \\ c-\chi \\ c-\chi \\ 0 \\ 0 \end{pmatrix} \tag{11}$$

It is not difficult to infer that all signalized intersections have similar formulas like Equations (8) and (11), which means that for each lane, its corresponding green time has a linear relationship with the independent control variables. Let $\boldsymbol{u} \in \mathbf{R}^m$ be the vector of all chosen independent control variables in the network. By combining the formulas of all intersections, the following relationship is obtained:

$$\boldsymbol{g} = \boldsymbol{G}\boldsymbol{u} + \boldsymbol{\xi} \tag{12}$$

where $\boldsymbol{G} \in \mathbf{R}^{n \times m}$ and $\boldsymbol{\xi} \in \mathbf{R}^n$.

Hence, the original store-and-forward model (5) can be restated as

$$\begin{aligned} \boldsymbol{x}(k+1) &= \boldsymbol{x}(k) + T\boldsymbol{r}(k) + \boldsymbol{L}(\boldsymbol{G}\boldsymbol{u}(k) + \boldsymbol{\xi}) \\ &= \boldsymbol{x}(k) + T\boldsymbol{r}(k) + \boldsymbol{L}\boldsymbol{G}\boldsymbol{u}(k) + \boldsymbol{L}\boldsymbol{\xi} \\ &= \boldsymbol{x}(k) + T\boldsymbol{r}(k) + \boldsymbol{B}\boldsymbol{u}(k) + \boldsymbol{h} \end{aligned} \tag{13}$$

where $\boldsymbol{B} = \boldsymbol{L}\boldsymbol{G} \in \mathbf{R}^{n \times m}$ and $\boldsymbol{h} = \boldsymbol{L}\boldsymbol{\xi} \in \mathbf{R}^n$. Now, we assume that availability of the nominal situation where a fixed signal control plan $\boldsymbol{g}^N$ (or equivalent $\boldsymbol{u}^N$) has been calculated by means of any fixed-time control method based on fixed (historical) demands $\boldsymbol{r}^N$ [7, 9]. Mathematically, it means $T\boldsymbol{r}^N + \boldsymbol{B}\boldsymbol{u}^N + \boldsymbol{h} = 0$, which infers

$$\boldsymbol{h} = -T\boldsymbol{r}^N - \boldsymbol{B}\boldsymbol{u}^N \tag{14}$$

Note that, in [10], for general transportation systems, some available procedures have been presented to estimate nominal parameters.

Hence, it follows from Equation (13) that

$$\begin{aligned} \boldsymbol{x}(k+1) &= \boldsymbol{x}(k) + T\boldsymbol{r}(k) + \boldsymbol{B}\boldsymbol{u}(k) - T\boldsymbol{r}^N - \boldsymbol{B}\boldsymbol{u}^N \\ &= \boldsymbol{x}(k) + T(\boldsymbol{r}(k) - \boldsymbol{r}^N) + \boldsymbol{B}(\boldsymbol{u}(k) - \boldsymbol{u}^N) \end{aligned} \tag{15}$$

Finally, defining $\boldsymbol{v}(k) = \boldsymbol{u}(k) - \boldsymbol{u}^N$ as the new control variable and defining $\boldsymbol{\omega} = T(\boldsymbol{r}(k) - \boldsymbol{r}^N)$ as the disturbances, Equation (15) yields the state-space model of our system

$$\boldsymbol{x}(k+1) = \boldsymbol{x}(k) + \boldsymbol{B}\boldsymbol{v}(k) + \boldsymbol{\omega}(k) \tag{16}$$

Apparently, by introducing the nominal situation, the term $\boldsymbol{\omega}$ has been defined as the differences between the real unknown traffic demands and the nominal ones. In other words, $\boldsymbol{\omega}$ reflects the unknown

DOI: 10.1002/atr

uncertainties in traffic demands that the fixed signal control plan $\boldsymbol{g}^N$ fails to consider. Hence, it is the disturbance that the H_∞ control method aims to attenuate.

Note that the state $\boldsymbol{x}$ and control $\boldsymbol{u}$ of such model should both verify their physical limitations. First, the effective green time of each phase must satisfy certain boundary conditions, that is,

$$g_{i,min} \leq g_i \leq g_{i,max}, \quad \forall i \in \{1, \cdots, n\} \tag{17}$$

or the equivalent vector form

$$\boldsymbol{g}_{min} \leq \boldsymbol{g} \leq \boldsymbol{g}_{max} \tag{18}$$

where $\boldsymbol{g}_{min} = [\boldsymbol{g}_{1,min}, \cdots, \boldsymbol{g}_{n,min}]^T$ and $\boldsymbol{g}_{max} = [\boldsymbol{g}_{1,max}, \cdots, \boldsymbol{g}_{n,max}]^T$ are, respectively, the well-selected minimal and maximal boundaries of $\boldsymbol{g}$. In view of Equation (12) and $\boldsymbol{v}(k) = \boldsymbol{u}(k) - \boldsymbol{u}^N$, these conditions on the green times infer the constraint set on the control variable $\boldsymbol{v}$ as follows:

$$\mathbb{U} = \{\boldsymbol{v} \in \mathbb{R}^m / \quad -\boldsymbol{v}_2 \leq \boldsymbol{G}\boldsymbol{v} \leq \boldsymbol{v}_1\} \tag{19}$$

where $\boldsymbol{v}_1 = \boldsymbol{g}_{max} - \boldsymbol{g}^N > 0$, $\boldsymbol{v}_2 = \boldsymbol{g}^N - \boldsymbol{g}_{min} > 0$ and $\boldsymbol{g}^N = \boldsymbol{G}\boldsymbol{u}^N + \xi$.

Furthermore, it makes no sense to speak of negative number of vehicles. Hence, we have $\boldsymbol{x}(k) \geq 0, \forall k \in \mathbb{N}$. On the other hand, each lane cannot contain infinite vehicles. We define the lane capacity as the maximal number of vehicles that a lane can contain. The transportation network model (16) is valid only when the number of vehicles in each lane does not exceed its capacity. Let x_i^*, $i \in \{1, \cdots, n\}$, be the capacity of lane i. The system (16) has physical meaning only if $\boldsymbol{x}$ belongs to the region of admissible states

$$\mathbb{X} = \{\boldsymbol{x} \in \mathbb{R}^n / \quad 0 \leq x \leq x^*\} \tag{20}$$

where $\boldsymbol{x}^* = \left[x_1^*, \cdots, x_n^*\right]^T$.

Now, to measure the performances of transportation network, the outputs of system need to be specified as the objective variable of robust control. The direct candidate is the number of vehicles $\boldsymbol{x}$: the fewer vehicles correspond to better performances. But, because the lane capacities are not all the same, the occupancies, which are the proportions between the number of vehicles and their capacities, are more suitable to show the system performances. Therefore, let $z_i = x_i / x_i^*$; then, the vector $\boldsymbol{z} = [z_1, \cdots, z_n]^T$ is the appropriate output variable of the system. Moreover, because the outputs of the cycle k should correspond to the states at instant $k+1$, $z_i(k)$ should equal to $x_i(k+1)/x_i^*$ instead of $x_i(k)/x_i^*$, $i \in \{1, \cdots, n\}$. Hence, the outputs of transportation system (16) are defined as

$$\boldsymbol{z}(k) = \boldsymbol{P}\boldsymbol{x}(k+1) = \boldsymbol{P}\boldsymbol{x}(k) + \boldsymbol{P}\boldsymbol{B}\boldsymbol{v}(k) + \boldsymbol{P}\boldsymbol{\omega}(k) \tag{21}$$

where $\boldsymbol{P}$ is the diagonal matrix with the diagonal elements $1/x_i^*$. Apparently, its constraint is given by

$$\mathbb{Z} = \{\boldsymbol{z} \in \mathbb{R}^n / \quad 0 \leq \boldsymbol{z} \leq 1\} \tag{22}$$

where $1 \triangleq [1, \cdots, 1]^T$. The subsequent robust study will focus on the influence of the disturbance $\boldsymbol{\omega}$ on this output $\boldsymbol{z}$.

3. CONTROLLABILITY STUDY

Before studying the control issue, the controllability of the previous model needs to be first considered. Indeed, according to Equation (16), the rank of controllability matrix is

$$\mu = rank\left(\boldsymbol{B} \ \ \boldsymbol{I}\boldsymbol{B} \cdots \boldsymbol{I}^{n-1}\boldsymbol{B}\right) = rank(\boldsymbol{B}) \tag{23}$$

DOI: 10.1002/atr

Because the number of lanes is obviously bigger than the number of independent control variables (e.g., Equations (8) and (11)) and $\boldsymbol{B} \in \mathbf{R}^{n \times m}$, we have

$$\mu = rank(\boldsymbol{B}) \leq min(m, n) = m < n \tag{24}$$

So, the transportation system described by Equation (16) is not completely controllable, and the controllability dimension is μ.

This analysis indicates that the traffic signals cannot completely control the transportation network, which matches the general experiences. Indeed, if the vehicles that enter the system are too many, the traffic signal control cannot prevent congestions no matter which control strategy is implemented. On the other hand, if there are very few vehicles, even the conventional fixed-time signal schedules can effectively evacuate the traffic.

To better understand this controllability problem, we consider now a simple intersection as shown in Figure 5. There are two conflict traffic movements and two phases corresponding to them. Suppose that the saturated flow rates in these two directions are the same ($s_1 = s_2 = s$), and the discrete-time step equals to the cycle, that is, $T = c$. It is easy to infer the dynamics of the number of vehicles as follows:

$$x_1(k+1) = x_1(k) + r_1(k)c - g_1(k)s \tag{25}$$

$$x_2(k+1) = x_2(k) + r_2(k)c - g_2(k)s \tag{26}$$

Because the sum of two green times $g_1(k) + g_2(k) = c - \chi$ is fixed, we have

$$x_1(k+1) + x_2(k+1) = x_1(k) + x_2(k) + r_1(k)c + r_2(k)c - (c - \chi)s \tag{27}$$

Obviously, the sum of vehicles in two lanes is irrelevant to the green time split; it depends only on the traffic demands. In other words, we cannot change the sum $x_1 + x_2$ by means of the green time split. Hence, the sum of two lanes is not controllable by the green time split. On the other hand, consider the difference between the two lanes

$$\begin{aligned} & x_1(k+1) - x_2(k+1) \\ = \; & x_1(k) - x_2(k) + r_1(k)c - r_2(k)c - g_1(k)s + g_2(k)s \\ = \; & x_1(k) - x_2(k) + r_1(k)c - r_2(k)c - g_1(k)s + (c - \chi - g_1(k))s \\ = \; & x_1(k) - x_2(k) + r_1(k)c - r_2(k)c + (c - \chi)s - 2g_1(k)s \end{aligned} \tag{28}$$

It is clear that the dynamic of $x_1 - x_2$ can be influenced by the green time split. Indeed, if the lane with more input vehicles obtains more green time, the number of vehicles in two lanes can approximate, and it will be less possible to generate congestions. The objective of the green time split control in this example should be to reduce the difference $x_1 - x_2$ to prevent congestions. In summary, in this simple intersection, $x_1 + x_2$ and $x_1 - x_2$ correspond respectively to the uncontrollable and controllable parts.

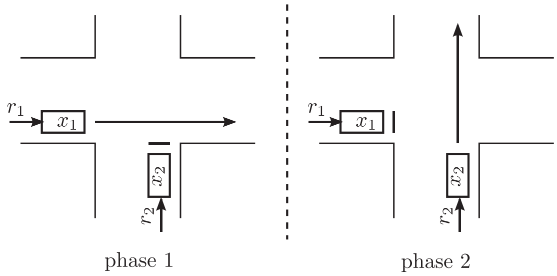

Figure 5. An intersection with two conflict flows.

DOI: 10.1002/atr

Furthermore, by comparing with the original store-and-forward model (5), the controllability problem of our model (16) is caused by the relationship (12). This relationship is imposed from the physical characteristics of the traffic signals (see Equations (8) and (11)); it must be satisfied to calculate admissible green times. Indeed, from $\boldsymbol{g}$ to $\boldsymbol{u}$, the dimension of control variables is reduced because of an important fact: for any intersection, the green time split can only regulate the unbalance between the lane groups corresponding to different phases. In other words, the power of the green time split is only to deal with the unbalance part of the system and to make the distribution of vehicles more uniformly such that the congestions can be prevented. This fact determines the lack of full controllability of the transportation network.

It is necessary to note that, in the existing works that have applied the store-and-forward approach (e.g., [7, 10, 19]), the relationship (12) is ignored in the modeling, and the system is considered controllable by using the control variable $\boldsymbol{g}$. However, such relationship is imposed by the physical signification; hence, it must be verified in the implementation of their proposed control strategies. For example, although the feedback control law of [7] is calculated without considering this relationship, its controller in real systems must solve a quadratic-programming (QP) problem in every cycle to obtain the most approximate green times that satisfy such condition. The effect of this QP problem has not been properly discussed, and the simulation study in Section 5 will show that this strategy has no effect on the uncontrollable part of the system either. Furthermore, Tettamanti *et al.* [19] applied a rolling-horizon control paradigm and considered such condition as a constraint of the optimization. In our opinion, this is actually equivalent to our approach that applies Equation (12) into the model, although it is not necessary for its rolling-horizon control paradigm to consider the controllability. Another notable work presented in [22] has also noticed the controllability problem. However, it avoided this problem by proposing an assumption that the number of phases is so big to fit the controllability demand, which, in our opinion, is unpractical.

In this paper, we choose to decompose the transportation network to isolate the completely controllable part, which determines the boundaries of the power of the green time split. In other words, the system (denoted by Σ) should be decomposed into two subsystems:

(1) the controllable subsystem with the dimension μ, which is completely controllable by $\boldsymbol{v}$, denoted by Σ_c; and
(2) the free subsystem with the dimension $(n-\mu)$, which is irrelevant with the control variable $\boldsymbol{v}$, denoted by Σ_u.

This is the emphasis of the following part.

3.1. Decomposition

Generally, the controllability decomposition relies on the controllability matrix. More precisely, the controllable space is the image of column space of controllability matrix. For the transportation system (16), this implies that Σ_c corresponds to the range of the matrix $\boldsymbol{B}^T$, denoted by

$$range\left(\boldsymbol{B}^T\right) = \left\{\boldsymbol{B}^T\boldsymbol{\theta}\in\mathbb{R}^m / \quad \forall\boldsymbol{\theta}\in\mathbb{R}^n\right\} \tag{29}$$

whose dimension equals $rank(\boldsymbol{B}^T) = \mu$. Hence, there exist μ linearly independent vectors, $\boldsymbol{\theta}_1, \cdots, \boldsymbol{\theta}_\mu \in \mathbb{R}^n$, such that $\{\boldsymbol{B}^T\boldsymbol{\theta}_1, \cdots, \boldsymbol{B}^T\boldsymbol{\theta}_\mu\}$ is a basis of $range(\boldsymbol{B}^T)$.

On the other hand, the free subsystem Σ_u corresponds to the null space of matrix $\boldsymbol{B}^T$, denoted by

$$null\left(\boldsymbol{B}^T\right) = \left\{\boldsymbol{\theta}\in\mathbb{R}^n / \quad \boldsymbol{B}^T\boldsymbol{\theta} = \boldsymbol{0}\right\} \tag{30}$$

whose dimension is $n-\mu$. Let $\{\boldsymbol{\theta}_{\mu+1}, \cdots, \boldsymbol{\theta}_n\}$ be a basis of $null(\boldsymbol{B}^T)$, and define two matrices as follows:

$$\boldsymbol{R}_1 = \left[\boldsymbol{\theta}_1, \cdots, , \boldsymbol{\theta}_\mu\right]\in\boldsymbol{R}^{n\times\mu} \tag{31}$$

$$\boldsymbol{R}_2 = \left[\boldsymbol{\theta}_{\mu+1}, \cdots, , \boldsymbol{\theta}_n\right]\in\mathbb{R}^{n\times(n-\mu)} \tag{32}$$

According to [23], these two matrices correspond to the two subsystems Σ_c and Σ_u. Note that there are infinite possible choices of the vectors, $\boldsymbol{\theta}_1$, $\cdots$, $\boldsymbol{\theta}_\mu$, $\boldsymbol{\theta}_{\mu+1}$, $\cdots$, $\boldsymbol{\theta}_n$. To conveniently perform the

DOI: 10.1002/atr

decomposition, we propose some additive conditions to choose them. Indeed, observe that the formula of output (21) includes the matrix P. Hence, it is better that the vectors $\boldsymbol{\theta}_i$, $i\in\{1,\cdots,n\}$, have some features related with this matrix. To do this, because $\boldsymbol{P}^{-1}$ is the diagonal matrix with diagonal elements x_i^*, it is easy to prove that the operator

$$<\boldsymbol{v},\boldsymbol{u}>_{\boldsymbol{P}}=\boldsymbol{v}^T\boldsymbol{P}^{-1}\boldsymbol{u},\forall\boldsymbol{v},\boldsymbol{u}\in\mathbb{R}^n \tag{33}$$

defines an inner product and $\mathbb{R}^n$ along with $<\cdot,\cdot>_{\boldsymbol{P}}$ is an inner product space. The orthogonality notion can be then redefined as

Definition 1.
[24] *The vectors,* $\boldsymbol{v},\boldsymbol{u}\in\mathbb{R}^n$, *are said to be orthogonal if* $<\boldsymbol{v},\boldsymbol{u}>_{\boldsymbol{P}}=\boldsymbol{v}^T\boldsymbol{P}^{-1}\boldsymbol{u}=0$.

With this new orthogonality, according to the Gram–Schmidt lemma ([24], page 108), there must be a choice of orthonormal vectors, $\boldsymbol{\theta}_1,\cdots,\boldsymbol{\theta}_\mu,\boldsymbol{\theta}_{\mu+1},\cdots,\boldsymbol{\theta}_n$, which means

$$<\boldsymbol{\theta}_i,\boldsymbol{\theta}_j>_{\boldsymbol{P}}=\boldsymbol{\theta}_i^T\boldsymbol{P}^{-1}\boldsymbol{\theta}_j=\begin{cases}0: i\neq j\\ 1: i=j\end{cases} \tag{34}$$

$\forall i,j\in\{1,\cdots,n\}$. From now on, we assume that the vectors $\boldsymbol{\theta}_i$, $i\in\{1,\cdots,n\}$, are orthonormal.

Now, we are prepared to prove the following facts for the subsequent development.

Fact 1
The matrices $\boldsymbol{R}_1$, $\boldsymbol{R}_2$ defined in Equations (31) and (32) verify

(1) $rank\left(\boldsymbol{R}_1^T\boldsymbol{B}\right)=\mu$;
(2) $\boldsymbol{R}_2^T\boldsymbol{B}=0$; and
(3) $\boldsymbol{P}=\boldsymbol{R}_1\boldsymbol{R}_1^T+\boldsymbol{R}_2\boldsymbol{R}_2^T$.

Proof.
First, from Equation (31), we have

$$\begin{aligned}R_1^TB&=\left[\theta_1,\cdots,\theta_\mu\right]^TB\\&=\left[\boldsymbol{B}^T\boldsymbol{\theta}_1,\cdots,\boldsymbol{B}^T\boldsymbol{\theta}_\mu\right]^T\in\mathbb{R}^{\mu\times m}\end{aligned} \tag{35}$$

Because $\{\boldsymbol{B}^T\boldsymbol{\theta}_1,\cdots,\boldsymbol{B}^T\boldsymbol{\theta}_\mu\}$ is a basis of $range(\boldsymbol{B}^T)$, these μ vectors are linearly independent. Hence, we have $rank\left(\boldsymbol{R}_1^T\boldsymbol{B}\right)=\mu$. Then, because $\{\boldsymbol{\theta}_{\mu+1},\cdots,\boldsymbol{\theta}_n\}$ is a basis of $null(\boldsymbol{B}^T)$, we have $\boldsymbol{B}^T\boldsymbol{\theta}_i=\boldsymbol{0}$, for $i\in\{\mu+1,\cdots,n\}$, which leads to $\boldsymbol{R}_2^T\boldsymbol{B}=0$. Finally, Equation (34) implies $(\boldsymbol{R}_1,\boldsymbol{R}_2)^T\boldsymbol{P}^{-1}(\boldsymbol{R}_1,\boldsymbol{R}_2)=\boldsymbol{I}$, which implies $\boldsymbol{P}^{-1}=((\boldsymbol{R}_1,\boldsymbol{R}_2)^T)^{-1}(\boldsymbol{R}_1,\boldsymbol{R}_2)^{-1}$. Hence, it follows

$$\begin{aligned}P&=(\boldsymbol{R}_1,\boldsymbol{R}_2)(\boldsymbol{R}_1,\boldsymbol{R}_2)^T\\&=\boldsymbol{R}_1\boldsymbol{R}_1^T+\boldsymbol{R}_2,\boldsymbol{R}_2^T\end{aligned} \tag{36}$$

The proof is completed.□

Now, define $\boldsymbol{x}_c=R_1^T\boldsymbol{x}\in\mathbb{R}^\mu$ (resp., $\boldsymbol{x}_u=R_2^T\boldsymbol{x}\in\mathbb{R}^{n-\mu}$) as the state variable of the controllable subsystem Σ_c (resp., free subsystem Σ_u). By multiplying the matrices $\boldsymbol{R}_1$ and $\boldsymbol{R}_2$, respectively, in the two sides of Equation (16), two subsystems are stated by the following expressions:

$$\Sigma_c:\boldsymbol{x}_c(k+1)=\boldsymbol{x}_c(k)+\boldsymbol{B}_c\boldsymbol{v}(k)+\boldsymbol{\omega}_c(k) \tag{37}$$

$$\Sigma_u:\boldsymbol{x}_u(k+1)=\boldsymbol{x}_u(k)+\boldsymbol{\omega}_u(k) \tag{38}$$

where $\boldsymbol{B}_c=\boldsymbol{R}_1^T\boldsymbol{B},\boldsymbol{\omega}_c=\boldsymbol{R}_1^T\boldsymbol{\omega}\in\mathbb{R}^\mu$ and $\boldsymbol{\omega}_u=\boldsymbol{R}_2^T\boldsymbol{\omega}\in\mathbb{R}^{n-\mu}$. The control constraint (19) remains unchanged. Furthermore, for the controlled outputs $\boldsymbol{z}$, we have in view of Equation (36)

DOI: 10.1002/atr

$$\begin{aligned} z(k) &= \boldsymbol{P}\boldsymbol{x}(k+1) \\ &= \boldsymbol{R}_1\boldsymbol{R}_1^T\boldsymbol{x}(k+1) + \boldsymbol{R}_2\boldsymbol{R}_2^T\boldsymbol{x}(k+1) \\ &= \boldsymbol{R}_1\boldsymbol{x}_c(k+1) + \boldsymbol{R}_2\boldsymbol{x}_u(k+1) \end{aligned} \tag{39}$$

Hence, the outputs of two subsystems are defined as

$$\begin{aligned} \Sigma_c : z_c(k) &= \boldsymbol{R}_1\boldsymbol{x}_c(k+1) \\ &= \boldsymbol{R}_1\boldsymbol{x}_c(k) + \boldsymbol{R}_1\boldsymbol{B}_c\boldsymbol{v}(k) + \boldsymbol{R}_1\boldsymbol{\omega}_c(k) \end{aligned} \tag{40}$$

$$\begin{aligned} \Sigma_u : z_u(k) &= \boldsymbol{R}_2\boldsymbol{x}_u(k+1) \\ &= \boldsymbol{R}_2\boldsymbol{x}_u(k) + \boldsymbol{R}_2\boldsymbol{\omega}_u(k) \end{aligned} \tag{41}$$

with $z = z_c + z_u$.

4. $\boldsymbol{H_\infty}$ CONTROL OF TRANSPORTATION SYSTEM

The objective of robust control is to reduce or limit the influences of the disturbances on the outputs in order to increase the system tolerance to the uncertainties. There are two popular approaches in robustness investigations that correspond to H_2 and H_∞ norms, respectively, of the transfer function from disturbances ($\boldsymbol{\omega}$) to outputs (z). H_2 norm measures the responds of system because of impulsive input, while H_∞ norm measures the least upper bound of $\| z \|_2/\| \boldsymbol{\omega} \|_2$ [25]. Clearly, the H_∞ norm is more strict and can guarantee better results, which is the major topic of most existing robustness studies [26].

Now, consider the controllable subsystem Σ_c with the difference Equation (37) and the output (40) as shown in Figure 6. If the state feedback control law

$$\boldsymbol{v}(k) = \boldsymbol{K}_c\boldsymbol{x}_c(k) \tag{42}$$

is chosen, where $\boldsymbol{K}_c$ is the feedback gain, we have the closed-loop expressions

$$\begin{aligned} \boldsymbol{x}_c(k+1) &= \boldsymbol{A}_{cl}\boldsymbol{x}_c(k) + \boldsymbol{\omega}_c(k) \\ z_c(k) &= \boldsymbol{C}_{cl}\boldsymbol{x}_c(k) + \boldsymbol{D}_{cl}\boldsymbol{\omega}_c(k) \end{aligned} \tag{43}$$

where $\boldsymbol{A}_{cl} = \boldsymbol{I} + \boldsymbol{B}_c\boldsymbol{K}_c$, $\boldsymbol{C}_{cl} = \boldsymbol{R}_1 + \boldsymbol{R}_1\boldsymbol{B}_c\boldsymbol{K}_c$ and $\boldsymbol{D}_{cl} = \boldsymbol{R}_1$.

Hence, the transfer function from $\boldsymbol{\omega}_c$ to $\boldsymbol{z}_c$ is given by

$$\boldsymbol{G}(z) = \boldsymbol{C}_{cl}(z\boldsymbol{I} - \boldsymbol{A}_{cl})^{-1} + \boldsymbol{D}_{cl} \tag{44}$$

The objective of H_∞ control is to find an appropriate feedback gain $\boldsymbol{K}_c$ such that H_∞ norm of $\boldsymbol{G}(z)$, which is denoted by $\| \boldsymbol{G}(z) \|_\infty$, is less than a given scalar $\gamma > 0$; this is equivalent to make

$$\|\boldsymbol{z}_c(k)\|_2 \le \gamma \|\boldsymbol{\omega}_c(k)\|_2, \quad \forall k \in \mathbb{N} \tag{45}$$

In the sequel, we will discuss its physical signification in transportation context.

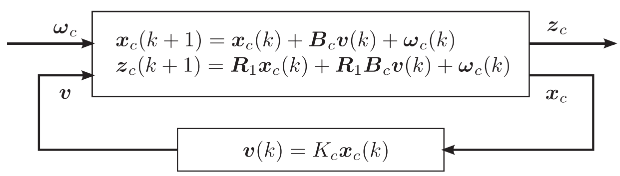

Figure 6. $\mathbf{H}_\infty$ problem of the controllable subsystem $\boldsymbol{\Sigma}_\mathbf{c}$.

Generally speaking, the objective of traffic signal control is to prevent congestions. Here, this objective is represented by the constraints on the outputs:

$$\mathbf{0} \leq z \leq \mathbf{1} \tag{46}$$

According to the controllability analysis, z is not fully controlled by the traffic lights, which includes two parts: the controllable outputs z_c and the uncontrollable ones z_u. The traffic signal control only has effects on z_c, while z_u is completely determined by $\boldsymbol{\omega}_u$. Hence, the control strategy should limit z_c as much as possible to verify the constraints on z. To do this, observe that, for each instant $k \in \mathbb{N}$, we have $z_c(k) = z(k) - z_u(k)$, which implies that if the controller makes

$$-z_u(k) \leq z_c(k) \leq 1 - z_u(k) \tag{47}$$

the constraints $\mathbf{0} \leq z(k) \leq \mathbf{1}$ are respected. Hence, in order to prevent congestions, the controller should make z_c inside the following region of admissible states

$$\mathbb{Z}_c^* = \{z_c \in \mathbb{R}^n / - z_u(k) \leq z_c(k) \leq \mathbf{1} - z_u(k), \forall k \in \mathbb{N}\} \tag{48}$$

However, the H_∞ norm of $\boldsymbol{G}(z)$ reflects the relationship between $\| \boldsymbol{\omega}_c \|_2$ and $\| z_c \|_2$. So, to show the signification of H_∞ control, we should find the boundary of $\| z_c \|_2$ that renders $z_c \in \mathbb{Z}_c^*$. The following lemma gives an answer to this problem.

Lemma 1.
Define the positive vector

$$z_c^* = \left(z_{c,1}^*, \cdots, z_{c,n}^*\right)^T \tag{49}$$

where

$$z_{c,i}^* = min\left\{ \left(z_{u,i}(k), 1 - z_{u,i}(k)\right) / \;\; \forall k \in \mathbb{N} \right\} \tag{50}$$

and let

$$\alpha = min\left\{ z_{c,i}^* / \;\; i \in \{1, \cdots, n\} \right\} \tag{51}$$

Then, the set

$$\mathbb{Z}_c = \{z_c \in \mathbb{R}^n / \|z_c(k)\|_2 \leq \alpha, \forall k \in \mathbb{N}\} \tag{52}$$

is a subset of $\mathbb{Z}_c^*$.

Proof.
For each instant $k \in \mathbb{N}$, if $\| z_c(k) \|_2 \leq \alpha$, it follows $-\alpha \leq z_{c,i} \leq \alpha$, $\forall i \in \{1, \cdots, n\}$, which implies

$$-z_c^* \leq -[\alpha, \cdots, \alpha]^T \leq z_c(k) \leq [\alpha, \cdots, \alpha]^T \leq z_c^* \tag{53}$$

Because $z_c^* \leq \mathbf{1} - z_u(k)$ and $z_c^* \leq z_u(k)$, it follows

$$-z_u(k) \leq z_c(k) \leq 1 - z_u(k) \tag{54}$$

and consequently, $z_c(k) \in \mathbb{Z}_c^*$. The proof is completed.□
Hence, in order to prevent congestions, it suffices that the traffic signal control makes $z_c(k) \in \mathbb{Z}_c$, $\forall k \in \mathbb{N}$.

DOI: 10.1002/atr

Now, observe that the H_∞ control strategy is to make

$$\|z_c(k)\|_2 \leq \gamma\|\boldsymbol{\omega}_c(k)\|_2 \tag{55}$$

for any $k \in \mathbb{N}$. So, if the disturbances $\boldsymbol{\omega}_c$ are inside the region

$$\Omega_c = \left\{\boldsymbol{\omega}_c \in \mathbb{R}^\mu / \|\boldsymbol{\omega}_c(k)\|_2 \leq \frac{\alpha}{\gamma}, \forall k \in \mathbb{N}\right\} \tag{56}$$

then $\boldsymbol{z}_c \in \mathbb{Z}_c$ is verified.

In summary, if the controller renders $\|\boldsymbol{G}(z)\|_\infty \leq \gamma$ and the disturbances satisfy $\boldsymbol{\omega}_c \in \Omega_c$, the constraint $\boldsymbol{z} \in \mathbb{Z}$ and the equivalent one $\boldsymbol{x} \in \mathbb{X}$ are both verified, which leads to the prevention of congestions. This implies that α/γ measures the tolerance of system to the disturbances $\boldsymbol{\omega}_c$. The robust traffic signal control should maximize α/γ. However, because α is determined by $\boldsymbol{z}_u$, which is not controllable by the traffic lights, it is nature that the traffic signal control should minimize γ in order to maximize α/γ.

So, by combining the constraint (19) on $\boldsymbol{v}$, we have the objective of the H_∞ control for the transportation system: find, if possible, a state feedback control law $\boldsymbol{v} = \boldsymbol{K}_c\boldsymbol{x}_c$, which minimizes γ under the conditions:

(1) $\|\boldsymbol{G}(z)\|_\infty \leq \gamma$;
(2) $\boldsymbol{v}(k) \in \mathbb{U}$, $\forall k \in \mathbb{N}$.

This is a constrained H_∞ control problem for the transportation network.

4.1. Problem solution

First, to address $\|\boldsymbol{G}(z)\|_\infty \leq \gamma$, the discrete-time version of strict bounded real lemma is needed.

Lemma 2.
[27] *Let* $\boldsymbol{M}(z) = \boldsymbol{C}(z\boldsymbol{I} - \boldsymbol{A})^{-1}\boldsymbol{B} + \boldsymbol{D}$; *then, the following statements are equivalent:*

(1) $\|\boldsymbol{M}(z)\|_\infty \leq 1$.
(2) There exists a $\boldsymbol{X} = \boldsymbol{X}^T \succ 0$ such that

$$\begin{pmatrix} \boldsymbol{A} & \boldsymbol{B} \\ \boldsymbol{C} & \boldsymbol{D} \end{pmatrix}^T \begin{pmatrix} \boldsymbol{X} & \boldsymbol{0} \\ \boldsymbol{0} & \boldsymbol{I} \end{pmatrix} \begin{pmatrix} \boldsymbol{A} & \boldsymbol{B} \\ \boldsymbol{C} & \boldsymbol{D} \end{pmatrix} - \begin{pmatrix} \boldsymbol{X} & \boldsymbol{0} \\ \boldsymbol{0} & \boldsymbol{I} \end{pmatrix} \preccurlyeq 0 \tag{57}$$

where $\succ 0$ (resp., $\preccurlyeq 0$) means that the matrix is positive definite (resp., negative semi-definite).

Now, observe that $\|\boldsymbol{G}(z)\|_\infty \leq \gamma$ is equivalent to

$$\left\|\frac{1}{\gamma}\boldsymbol{C}_{cl}(z\boldsymbol{I} - \boldsymbol{A}_{cl})^{-1} + \frac{1}{\gamma}\boldsymbol{D}_{cl}\right\|_\infty \leq 1 \tag{58}$$

Hence, in view of Lemma 2, a necessary and sufficient condition of the solution of H_∞ control problem for transportation network is the existence of a matrix $X = X^T \succ 0$ such that

$$\begin{pmatrix} \boldsymbol{A}_{cl} & \boldsymbol{I} \\ \boldsymbol{C}_{cl} & \boldsymbol{D}_{cl} \end{pmatrix}^T \begin{pmatrix} \boldsymbol{X} & \boldsymbol{0} \\ \boldsymbol{0} & \gamma^{-2}\boldsymbol{I} \end{pmatrix} \begin{pmatrix} \boldsymbol{A}_{cl} & \boldsymbol{I} \\ \boldsymbol{C}_{cl} & \boldsymbol{D}_{cl} \end{pmatrix} - \begin{pmatrix} \boldsymbol{X} & \boldsymbol{0} \\ \boldsymbol{0} & \boldsymbol{I} \end{pmatrix} \preccurlyeq 0 \tag{59}$$

According to the Schur complement lemma [28], this inequality is equivalent to

DOI: 10.1002/atr

$$\begin{pmatrix} \boldsymbol{X} & * & * & * \\ 0 & \boldsymbol{I} & * & * \\ \boldsymbol{A}_{cl} & \boldsymbol{I} & \boldsymbol{X}^{-1} & * \\ \boldsymbol{C}_{cl} & \boldsymbol{D}_{cl} & \boldsymbol{0} & \gamma^2\boldsymbol{I} \end{pmatrix} \succcurlyeq 0 \tag{60}$$

where * represents the transpose of the elements across the diagonal. Now, define

$$\boldsymbol{M} = \begin{pmatrix} \sqrt{\gamma}\boldsymbol{I} & \boldsymbol{0} & \boldsymbol{0} & \boldsymbol{0} \\ \boldsymbol{0} & \sqrt{\gamma}\boldsymbol{I} & \boldsymbol{0} & \boldsymbol{0} \\ \boldsymbol{0} & \boldsymbol{0} & \frac{1}{\sqrt{\gamma}}\boldsymbol{I} & \boldsymbol{0} \\ \boldsymbol{0} & \boldsymbol{0} & \boldsymbol{0} & \frac{1}{\sqrt{\gamma}}\boldsymbol{I} \end{pmatrix} \tag{61}$$

Obviously, $\boldsymbol{M}$ is an invertible matrix. Hence, Equation (60) is equivalent to

$$\boldsymbol{M}^T \begin{pmatrix} \boldsymbol{X} & * & * & * \\ \boldsymbol{0} & \boldsymbol{I} & * & * \\ \boldsymbol{A}_{cl} & \boldsymbol{I} & \boldsymbol{X}^{-1} & * \\ \boldsymbol{C}_{cl} & \boldsymbol{D}_{cl} & \boldsymbol{0} & \gamma^2\boldsymbol{I} \end{pmatrix} \boldsymbol{M} \succcurlyeq 0 \tag{62}$$

which infers

$$\begin{pmatrix} \boldsymbol{Q} & * & * & * \\ \boldsymbol{0} & \gamma\boldsymbol{I} & * & * \\ \boldsymbol{A}_{cl} & \boldsymbol{I} & \boldsymbol{Q}^{-1} & * \\ \boldsymbol{C}_{cl} & \boldsymbol{D}_{cl} & \boldsymbol{0} & \gamma\boldsymbol{I} \end{pmatrix} \succcurlyeq 0 \tag{63}$$

where $\boldsymbol{Q} = \gamma\boldsymbol{X}$. This inequality is the necessary and sufficient condition for $\| \boldsymbol{G}(z) \|_\infty \le \gamma$. Summarizing, we have the following theorem.

Theorem 1.
For the system (37) with the output (40), the existence of a matrix $\boldsymbol{K}_c$ solution of the inequality

$$\begin{pmatrix} \boldsymbol{Q} & * & * & * \\ \boldsymbol{0} & \gamma\boldsymbol{I} & * & * \\ \boldsymbol{I} + \boldsymbol{B}_c\boldsymbol{K}_c & \boldsymbol{I} & \boldsymbol{Q}^{-1} & * \\ \boldsymbol{R}_1 + \boldsymbol{R}_1\boldsymbol{B}_c\boldsymbol{K}_c & \boldsymbol{R}_1 & \boldsymbol{0} & \gamma\boldsymbol{I} \end{pmatrix} \succcurlyeq 0 \tag{64}$$

is a necessary and sufficient condition for the existence of the control law $\boldsymbol{v} = \boldsymbol{K}_c\boldsymbol{x}_c$ that renders $\| z_c \|_2 / \|\boldsymbol{\omega}_c \|_2 \le \gamma$.

Now, once the gain matrix $\boldsymbol{K}_c$ is found, the feedback control should not violate the constraint (19). In view of $\boldsymbol{v} = \boldsymbol{K}_c\boldsymbol{x}_c = \boldsymbol{K}_c\boldsymbol{R}_1^T x$, the constraint set $\mathbb{U}$ is equivalent to

$$\mathbb{U}_x = \left\{ \boldsymbol{x} / \quad -\boldsymbol{v}_2 \le \boldsymbol{G}\boldsymbol{K}_c\boldsymbol{R}_1^T x \le v_1 \right\} \tag{65}$$

Hence, $\boldsymbol{v} \in \mathbb{U}$ requires that every trajectory $\boldsymbol{x}(k; \boldsymbol{x}(0))$ inside the region $\mathbb{X}$ does not leave $\mathbb{U}_x$ for any instant $k \in \mathbb{N}$. Consequently, the problem now consists in finding additional conditions on $\boldsymbol{K}_c$ such that

DOI: 10.1002/atr

$$\mathbb{X} \subseteq \mathbb{U}_x \tag{66}$$

To make the idea clear, the sets $\mathbb{X}$ and $\mathbb{U}_x$ are restated as the following general polyhedron forms, respectively,

$$\mathbb{X} = \left\{ \boldsymbol{x} / \quad \begin{bmatrix} \boldsymbol{I} \\ -\boldsymbol{I} \end{bmatrix} \boldsymbol{x} \le \begin{bmatrix} \boldsymbol{x}^* \\ \boldsymbol{0} \end{bmatrix} \right\} \tag{67}$$

$$\mathbb{U}_x = \left\{ \boldsymbol{x} / \quad \begin{bmatrix} \boldsymbol{G}\boldsymbol{K}_c\boldsymbol{R}_1^T \\ -\boldsymbol{G}\boldsymbol{K}_c\boldsymbol{R}_1^T \end{bmatrix} \boldsymbol{x} \le \begin{bmatrix} \boldsymbol{v}_1 \\ \boldsymbol{v}_2 \end{bmatrix} \right\} \tag{68}$$

According to the extension of Farkas' lemma in [29], the necessary and sufficient condition for verifying (66) is the existence of the non-negative matrix $\mathbb{T}$ with appropriate dimension such that

$$\mathbb{T} \begin{bmatrix} \boldsymbol{I} \\ -\boldsymbol{I} \end{bmatrix} = \begin{bmatrix} \boldsymbol{G}\boldsymbol{K}_c\boldsymbol{R}_1^T \\ -\boldsymbol{G}\boldsymbol{K}_c\boldsymbol{R}_1^T \end{bmatrix} \tag{69}$$

$$\mathbb{T} \begin{bmatrix} \boldsymbol{x}^* \\ \boldsymbol{0} \end{bmatrix} \le \begin{bmatrix} \boldsymbol{v}_1 \\ \boldsymbol{v}_2 \end{bmatrix} \tag{70}$$

Let

$$\mathbb{T} = \begin{bmatrix} \mathbb{T}_{11} & \mathbb{T}_{12} \\ \mathbb{T}_{21} & \mathbb{T}_{22} \end{bmatrix}$$

where $\mathbb{T}_{ij} \in \mathbb{R}^{m \times n}$. It follows that the linear conditions (69) and (70) are equivalent to

$$\mathbb{T}_{11} - \mathbb{T}_{12} = \mathbb{T}_{22} - \mathbb{T}_{21} = \boldsymbol{G}\boldsymbol{K}_c\boldsymbol{R}_1^T \tag{71}$$

$$\mathbb{T}_{11}\boldsymbol{x}^* \le \boldsymbol{v}_1 \tag{72}$$

$$\mathbb{T}_{21}\boldsymbol{x}^* \le \boldsymbol{v}_2 \tag{73}$$

In order to simplify these linear conditions and to reduce the number of variables, the following lemma is needed.

Lemma 3.
For any matrix $\boldsymbol{M}$, *define*

$$\begin{aligned} \boldsymbol{M}^+ &= \left(m_{ij}^+\right), \text{ where } m_{ij}^+ = sup\left(m_{ij}, 0\right) \\ \boldsymbol{M}^- &= \left(m_{ij}^-\right), \text{ where } m_{ij}^- = -inf\left(m_{ij}, 0\right) = sup\left(-m_{ij}, 0\right) \end{aligned}$$

If two non-negative matrices $\boldsymbol{A}$ and $\boldsymbol{B}$ with the same dimension of $\boldsymbol{M}$ verify that $\boldsymbol{A} - \boldsymbol{B} = \boldsymbol{M}$, then

$$\boldsymbol{A} \ge \boldsymbol{M}^+ \text{ and } \boldsymbol{B} \ge \boldsymbol{M}^- \tag{74}$$

Proof.

Observe that $\boldsymbol{A}-\boldsymbol{B}=\boldsymbol{M}$ implies $a_{ij}-b_{ij}=m_{ij}$. By definition, if $m_{ij}\geq 0$, we have $m_{ij}^{+}=m_{ij}$ and $m_{ij}^{-}=0$. Because $b_{ij}\geq 0$ and $a_{ij}-b_{ij}=m_{ij}$, it follows $b_{ij}\geq m_{ij}^{-}$ and $a_{ij}=b_{ij}+m_{ij}\geq m_{ij}=m_{ij}^{+}$; this implies that $\boldsymbol{A}\geq\boldsymbol{M}^{+}$ and $\boldsymbol{B}\geq\boldsymbol{M}^{-}$. On the other hand, if $m_{ij}<0$, we have $m_{ij}^{+}=0$ and $m_{ij}^{-}=-m_{ij}$. Because $a_{ij}\geq 0$ and $a_{ij}-b_{ij}=m_{ij}$, then $a_{ij}\geq m_{ij}^{+}$ and $b_{ij}=a_{ij}-m_{ij}\geq -m_{ij}=m_{ij}^{-}$; this also leads to $\boldsymbol{A}\geq\boldsymbol{M}^{+}$ and $\boldsymbol{B}\geq\boldsymbol{M}^{-}$. The proof is completed. □

Now, we are prepared to prove the following theorem.

Theorem 2.

The necessary and sufficient condition to verify the inclusion (66) is the existence of two non-negative matrices $\boldsymbol{N}_1$ and $\boldsymbol{N}_2$ *such that*

$$\boldsymbol{N}_1-\boldsymbol{N}_2=\boldsymbol{G}\boldsymbol{K}_c\boldsymbol{R}_1^T \tag{75}$$

$$\boldsymbol{N}_1\boldsymbol{x}^*\leq\boldsymbol{v}_1 \tag{76}$$

$$\boldsymbol{N}_2\boldsymbol{x}^*\leq\boldsymbol{v}_2 \tag{77}$$

Proof.

Sufficiency: It can be obtained by simply letting

$$\mathbb{T}=\begin{pmatrix}\boldsymbol{N}_1 & \boldsymbol{N}_2\\ \boldsymbol{N}_2 & \boldsymbol{N}_1\end{pmatrix} \tag{78}$$

Necessity: In view of Lemma 3, Equation (71) implies

$$\begin{matrix}\mathbb{T}_{11}\geq\left(\boldsymbol{G}\boldsymbol{K}_c\boldsymbol{R}_1^T\right)^{+} & \mathbb{T}_{22}\geq\left(\boldsymbol{G}\boldsymbol{K}_c\boldsymbol{R}_1^T\right)^{+}\\ \mathbb{T}_{12}\geq\left(\boldsymbol{G}\boldsymbol{K}_c\boldsymbol{R}_1^T\right)^{-} & \mathbb{T}_{21}\geq\left(\boldsymbol{G}\boldsymbol{K}_c\boldsymbol{R}_1^T\right)^{-}\end{matrix} \tag{79}$$

This and Equations (72) and (73) infer

$$\left(\boldsymbol{G}\boldsymbol{K}_c\boldsymbol{R}_1^T\right)^{+}\boldsymbol{x}^*\leq\mathbb{T}_{11}\boldsymbol{x}^*\leq\boldsymbol{v}_1 \tag{80}$$

$$\left(\boldsymbol{G}\boldsymbol{K}_c\boldsymbol{R}_1^T\right)^{-}\boldsymbol{x}^*\leq\mathbb{T}_{21}\boldsymbol{x}^*\leq\boldsymbol{v}_2 \tag{81}$$

Hence, the necessity can be proven by letting

$$\boldsymbol{N}_1=\left(\boldsymbol{G}\boldsymbol{K}_c\boldsymbol{R}_1^T\right)^{+} \tag{82}$$

$$\boldsymbol{N}_2=\left(\boldsymbol{G}\boldsymbol{K}_c\boldsymbol{R}_1^T\right)^{-} \tag{83}$$

The proof is completed. □

Summarizing, Theorems 1 and 2 present, respectively, the necessary and sufficient conditions on $\boldsymbol{K}_c$ to verify $\|\boldsymbol{G}(z)\|_\infty\leq\gamma$ and the constraints on $\boldsymbol{v}(k)$. Hence, by combining them, we are now in the position to present the final result of the H_∞ optimal traffic signal control strategy for the transportation system.

DOI: 10.1002/atr

Theorem 3.
For the controllable subsystem (37) with the output (40), if the feedback gain $\boldsymbol{K}_c$, *the positive definite matrix* $\boldsymbol{Q}$, *the non-negative matrices* $\boldsymbol{N}_1$ and $\boldsymbol{N}_2$, *and the positive scalar* γ *are solutions of the following optimization problem*

$$\begin{gathered} min\ \gamma \\ \text{subject to } (64) \text{ and } (75)-(77) \end{gathered} \tag{84}$$

then the feedback control $\boldsymbol{v}=\boldsymbol{K}_c\boldsymbol{x}_c$ guarantees the following statements:

(1) $\| z_c \|_2/\|\boldsymbol{\omega}_c\|_2 \leq \gamma$;
(2) $\boldsymbol{v}(k)\in\mathbb{U}$, for any $k\in\mathbb{N}$.

It is important to note that the solvability of the optimization problem (84) is a hard problem because of the nonlinear element $\boldsymbol{Q}^{-1}$ in Equation (64). Indeed, Equations (64) and 75–77 are equivalent to

$$\begin{pmatrix} \hat{\boldsymbol{Q}} & * & * & * \\ \boldsymbol{0} & \gamma\boldsymbol{I} & * & * \\ \hat{\boldsymbol{Q}}+\boldsymbol{B}_c\boldsymbol{Y} & \boldsymbol{I} & \hat{\boldsymbol{Q}} & * \\ \boldsymbol{R}_1\hat{\boldsymbol{Q}}+\boldsymbol{R}_1\boldsymbol{B}_c\boldsymbol{Y} & \boldsymbol{R}_1 & \boldsymbol{0} & \gamma\boldsymbol{I} \end{pmatrix} \succcurlyeq 0 \tag{85}$$

$$\begin{cases} -\boldsymbol{N}_2 - \boldsymbol{GYQR}_1^T \leq 0 \\ \boldsymbol{GYQR}_1^T x^* + \boldsymbol{N}_2 x^* - v_1 \leq 0 \\ \boldsymbol{N}_2 x^* - v_2 \leq 0 \end{cases} \tag{86}$$

$$\hat{\boldsymbol{Q}}\boldsymbol{Q} = \boldsymbol{I} \tag{87}$$

where $\boldsymbol{Q}=\boldsymbol{Q}^{-1}$ and $\boldsymbol{Y}=\boldsymbol{K}_c\boldsymbol{Q}^{-1}$. Now, if we define the function $f_1(\boldsymbol{Q})$ that returns the diagonal matrix where the diagonal elements are all components of the matrix $\left(-\boldsymbol{N}_2 - \boldsymbol{GYQR}_1^T\right)$ and the vectors $\left(\boldsymbol{GYQR}_1^T x^* + \boldsymbol{N}_2\boldsymbol{x}^* - v_1\right)$, $(\boldsymbol{N}_2\boldsymbol{x}^* - v_2)$, then Equation (86) is equivalent to $f_1(\boldsymbol{Q}) \preccurlyeq 0$. Furthermore, define the matrix function as

$$f_2(\hat{\boldsymbol{Q}}) = -\begin{pmatrix} \hat{\boldsymbol{Q}} & * & * & * \\ \boldsymbol{0} & \gamma\boldsymbol{I} & * & * \\ \hat{\boldsymbol{Q}}+\boldsymbol{B}_c\boldsymbol{Y} & \boldsymbol{I} & \hat{\boldsymbol{Q}} & * \\ \boldsymbol{R}_1\hat{\boldsymbol{Q}}+\boldsymbol{R}_1\boldsymbol{B}_c\boldsymbol{Y} & \boldsymbol{R}_1 & \boldsymbol{0} & \gamma\boldsymbol{I} \end{pmatrix} \tag{88}$$

Then, the conditions 85–87 can be equivalently rewritten as

$$f_1(\boldsymbol{Q})\preccurlyeq 0,\ \ f_2(\hat{\boldsymbol{Q}})\preccurlyeq 0,\ \ \hat{\boldsymbol{Q}}\boldsymbol{Q} = \boldsymbol{I} \tag{89}$$

This problem has been proven to be an Non-deterministic Polynomial (NP)-hard problem in [30]; hence, the computational efficiency of (84) cannot be guaranteed.

To overcome this difficulty, for our optimization problem, we can choose $\boldsymbol{Q}=\boldsymbol{I}$. In this case, Equation (64) becomes

$$\begin{pmatrix} \boldsymbol{I} & * & * & * \\ \boldsymbol{0} & \gamma\boldsymbol{I} & * & * \\ \boldsymbol{I}+\boldsymbol{B}_c\boldsymbol{K}_c & \boldsymbol{I} & \boldsymbol{I} & * \\ \boldsymbol{R}_1+\boldsymbol{R}_1\boldsymbol{B}_c\boldsymbol{K}_c & \boldsymbol{R}_1 & \boldsymbol{0} & \gamma\boldsymbol{I} \end{pmatrix} \succcurlyeq 0 \tag{90}$$

which is a linear matrix inequality (LMI), and it is only a sufficient (but not necessary) condition for $\| \boldsymbol{G}(z) \|_\infty \leq \gamma$. This leads to the following corollary.

DOI: 10.1002/atr

Corollary 1.
For the controllable subsystem (37) with the output (40), if the feedback gain $\boldsymbol{K}_c$, the non-negative matrices $\boldsymbol{N}_1$ and $\boldsymbol{N}_2$, and the positive scalar γ are solutions of the following optimization problem

$$\min \ \gamma$$
$$\text{subject to}$$
$$LMI \ : \begin{pmatrix} \boldsymbol{I} & * & * & * \\ \boldsymbol{0} & \gamma\boldsymbol{I} & * & * \\ \boldsymbol{I}+\boldsymbol{B}_c\boldsymbol{K}_c & \boldsymbol{I} & \boldsymbol{I} & * \\ \boldsymbol{R}_1+\boldsymbol{R}_1\boldsymbol{B}_c\boldsymbol{K}_c & \boldsymbol{R}_1 & \boldsymbol{0} & \gamma\boldsymbol{I} \end{pmatrix} \succcurlyeq 0 \tag{91}$$

$$\begin{aligned} &\boldsymbol{N}_1-\boldsymbol{N}_2=\boldsymbol{K}_c\boldsymbol{R}_1^T \\ &\boldsymbol{N}_1\boldsymbol{x}^*\leq\boldsymbol{v}_1 \\ &\boldsymbol{N}_2\boldsymbol{x}^*\leq\boldsymbol{v}_2 \end{aligned} \tag{92}$$

then the feedback control $v=\boldsymbol{K}_c\boldsymbol{x}_c$ guarantees the following statements:

(1) $\| z_c \|_2/\| \boldsymbol{\omega}_c \|_2\leq\gamma$;
(2) $\boldsymbol{v}(k)\in\mathbb{U}$, for any $k\in\mathbb{N}$.

This corollary transforms the problem into a convex programming problem with LMI and linear conditions, which can be efficiently solved by using standard numerical tools like MATLAB [31, 32]. However, by using $\boldsymbol{Q}=\boldsymbol{I}$, the optimal solution γ^* of Corollary 1 is only sub-optimal with respect to the true optimal solution of Theorem 3. This is a trade-off between the efficiency and the performance.

5. SIMULATION STUDY

The simulation study on a large-scale hypothetical network taken from [33] (Figure 7) is conducted in this section to demonstrate the comparative power of the proposed method. More precisely, we

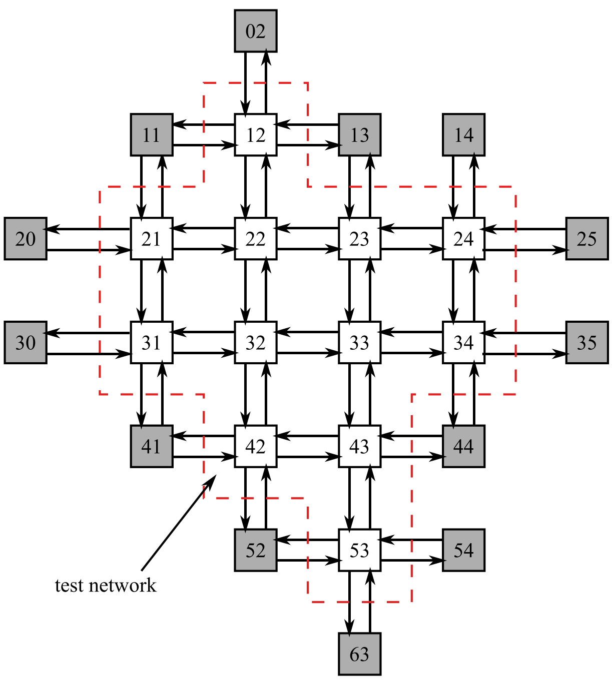

Figure 7. Hypothetical test network [33].

DOI: 10.1002/atr

compare the closed-loop behaviors of the constrained H_∞ controller and the linear-quadratic (LQ) method proposed in [7]. To ensure fair and comparable results, both methodologies are evaluated by the use of the same simulation models. More precisely, two simulation models are applied: the original store-and-forward model (5) and the CTM introduced in [4].

5.1. Characteristics

The core area of the test network consists of 12 intersections numbered 12, 21, 22, 23, 24, 31, 32, 33, 34, 42, 43 and 54, respectively. Among them, intersections 21, 33 and 53 function with a two-phase signal system as shown in Figure 3, while the others are with a four-phase signal system as in Figure 8. We assume that all intersections share the same cycle time $c = 100$ s, and $T = c$ is taken as the discrete-time step. For each phase of the two-phase signal system, the lost time is assumed as 5 s; the minimal and maximal values of the effective green time are $0.3(c-\chi)$ and $0.7(c-\chi)$, where χ is the total lost time of the corresponding intersection in one cycle. For the intersections with the four-phase signal system, the lost times are set to be 5, 3, 5 and 3 s, respectively, and the effective green times are bounded between $0.25(c-\chi)$, $0.07(c-\chi)$, $0.25(c-\chi)$, $0.07(c-\chi)$ and $0.55(c-\chi)$, $0.15(c-\chi)$, $0.55(c-\chi)$, $0.15(c-\chi)$, respectively. The details of the parameters of the links in the test area are listed in Table I. The capacities x_i^* are derived by considering the average vehicle length as 5 m. The turning rates are given based on the assumption that, for each horizontal link, the percentages of the vehicles turning left and right are both set to be 0.1; on the other hand, for each vertical link, the turning rates to left and right are equal to 0.2 and 0.3, respectively. Thus, the values of the matrices L, B and the vector h can be derived from these parameters.

The nominal values of the green times $\boldsymbol{g}^N$ as well as $\boldsymbol{u}^N$ are given in the following manners:

- For each two-phase intersection, the two phases both occupy half of the cycle time;
- For each four-phase intersection, the four green times are set to be $0.41(c-\chi)$, $0.09(c-\chi)$, $0.4(c-\chi)$ and $0.1(c-\chi)$, respectively.

Thus, the nominal demands $\boldsymbol{r}^N$ can be inferred from $\boldsymbol{Tr}^N + \boldsymbol{Bu}^N + \boldsymbol{h} = 0$.

5.2. Scenarios

Two scenarios are considered in the following simulations. The first one is the nominal situation, which has no disturbance during the simulation, that is, $\omega \equiv 0$. On the other hand, in order to illustrate the behaviors of the control methods in the presence of the disturbances, the second scenario adds sinusoidal

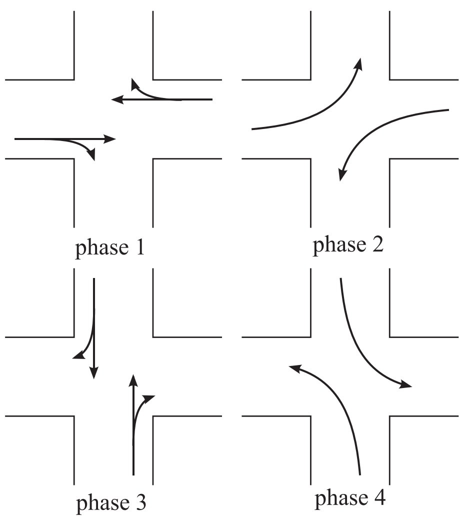

Figure 8. Four-phase signal system with left-turn protection control.

DOI: 10.1002/atr

Table I. Parameters of the links.

Links	Length (m)	Number of lanes	Saturation rate s_i (veh/s)	Exit rate
$11 \to 12$, $13 \to 12$	300	3	0.4	0
$20 \to 21$, $25 \to 24$	300	3	0.4	0
$30 \to 31$, $35 \to 34$	300	3	0.4	0
$41 \to 42$, $44 \to 43$	300	3	0.4	0
$52 \to 53$, $54 \to 53$	300	3	0.4	0
$21 \to 22$, $22 \to 21$	535	3	0.4	0.1
$22 \to 23$, $23 \to 22$	580	3	0.4	0.1
$23 \to 24$, $24 \to 23$	590	3	0.4	0.1
$31 \to 32$, $32 \to 31$	520	3	0.4	0.1
$32 \to 33$, $33 \to 32$	360	3	0.4	0.1
$33 \to 34$, $34 \to 33$	460	3	0.4	0.1
$42 \to 43$, $43 \to 42$	565	3	0.4	0.1
$11 \to 21$, $41 \to 31$	300	2	0.3	0
$02 \to 12$, $52 \to 42$	300	2	0.3	0
$13 \to 23$, $63 \to 53$	300	2	0.3	0
$14 \to 24$, $44 \to 34$	300	2	0.3	0
$21 \to 31$, $31 \to 21$	370	2	0.3	0.1
$12 \to 22$, $22 \to 12$	355	2	0.3	0.1
$22 \to 32$, $32 \to 22$	440	2	0.3	0.1
$32 \to 42$, $42 \to 32$	550	2	0.3	0.1
$23 \to 33$, $33 \to 23$	530	2	0.3	0.1
$33 \to 43$, $43 \to 33$	400	2	0.3	0.1
$43 \to 53$, $53 \to 43$	540	2	0.3	0.1
$24 \to 34$, $34 \to 24$	505	2	0.3	0.1

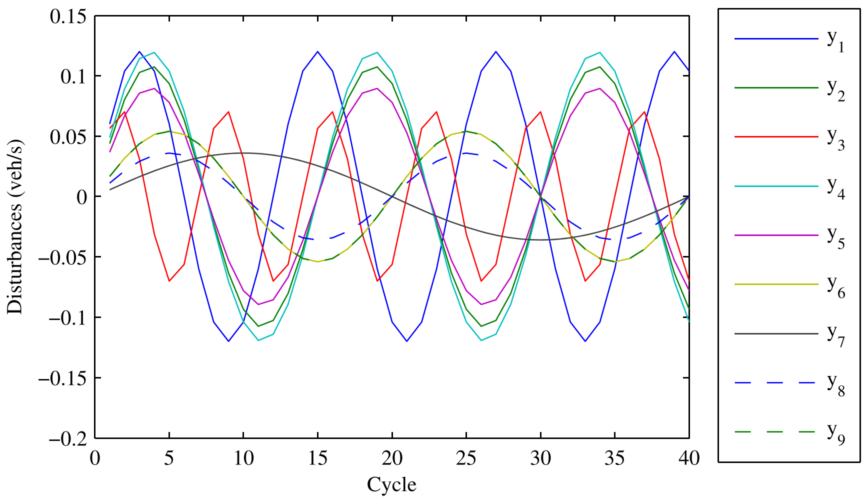

y_1 for $11 \to 12$ and $13 \to 12$ y_2 for $20 \to 21$ and $25 \to 24$
y_3 for $30 \to 31$ and $35 \to 34$ y_4 for $41 \to 42$ and $44 \to 43$
y_5 for $52 \to 53$ and $54 \to 53$ y_6 for $11 \to 21$ and $41 \to 31$
y_7 for $02 \to 12$ and $52 \to 42$ y_8 for $13 \to 23$ and $63 \to 53$
y_9 for $14 \to 24$ and $44 \to 34$

Figure 9. Patterns of disturbances.

uncertainties in every entry of the network with different amplitudes and frequencies. Detailed patterns of the flow rates of these disturbances are displayed in Figure 9. Note that, except the traffic demands, the two scenarios share the same conditions including the initial state $x(0)$.

DOI: 10.1002/atr

5.3. Comparison of criteria

For each scenario and for each control approach, three evaluation criteria are calculated for the comparison [5, 9]: the total time spent

$$\mathrm{TTS}(k) = T\sum_i x_i(k), \quad (\text{veh}\cdot\text{s}) \tag{93}$$

the relative queue balance

$$\mathrm{RQB}(k) = \sum_i \frac{x_i(k)^2}{x_i^*}, \quad (\text{veh}) \tag{94}$$

and the total delay (TD) of all vehicles in every cycle. Note that the TD can be only calculated by the use of the CTM.

Table II gives the average values of these three criteria in every case. It is clear that the constrained H_∞ control leads to a reduction of all evaluation criteria compared with the LQ approach for each scenario and each simulation model. Furthermore, we also observe that the improvements in the presence of the disturbances (scenario 2) are greater than the nominal situation (scenario 1). This fact implies that the constraint H_∞ control is more powerful to attenuate disturbances.

Another observation is that the performances from the CTM are worse than the store-and-forward model. The reason may be that the store-and-forward approach significantly simplifies the system model and leads to "ideal" results, while the CTM is more close to the real situations. Nevertheless, their differences do not change our conclusions.

Furthermore, note that our H_∞ control method decomposes the system and only focuses on the controllable part, but the LQ approach considers the system fully controllable. Hence, it is necessary to examine the power of the LQ approach on the part that we consider uncontrollable. Figure 10 shows the norm of the uncontrollable output $\| z_u \|_2$ in two scenarios. Observe that the two methodologies always lead to the same (nearly same) curves. Indeed, they are overlapped in most of the time. Specially in scenario 1, because there are no disturbances, the uncontrollable outputs stay unchanged during the entire simulation. It follows from this observation that, although the LQ method considers the system controllable, it cannot actually affect the uncontrollable part described in this paper either.

5.4. Effect of disturbances

The H_∞ method is designed for disturbance attenuation. Hence, the effect of disturbances (in scenario 2) on the controllable subsystem of the test network is illustrated in this part. It is observed from Figure 11 that the proposed H_∞ control method reduces such effect rapidly in the first 5 cycles and

Table II. Comparison of the criteria.

	Store and forward		CTM		
	TTS	RQB	TTS	RQB	TD
Scenario 1					
LQ	5.158e5	1.352e3	5.212e5	1.388e3	4.321e5
H_∞	5.026e5	1.321e3	5.071e5	1.352e3	4.162e5
Improvement	−2.63%	−2.3%	−2.79%	−2.68%	−3.82%
Scenario 2					
LQ	5.514e5	1.572e3	5.567e5	1.615e3	4.677e5
H_∞	5.356e5	1.524e3	5.388e5	1.552e3	4.501e5
Improvement	−2.95%	−3.14%	−3.33%	−4.07%	−3.91%

CTM, cell transmission model; TTS, total time spent; RQB, relative queue balance; TD, total delay.

DOI: 10.1002/atr

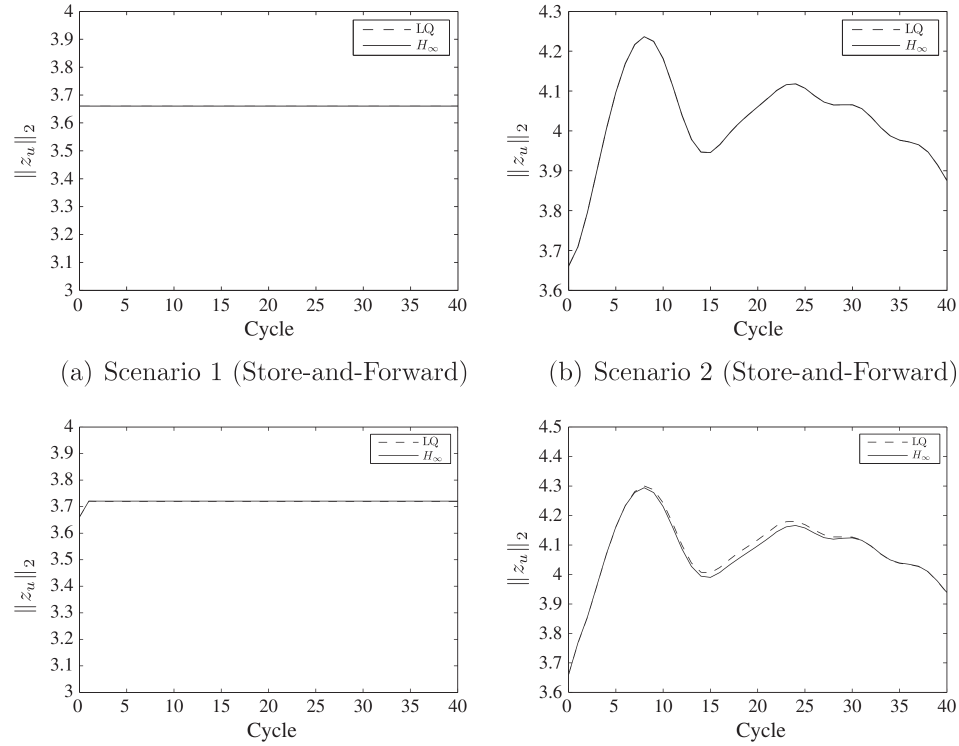

(a) Scenario 1 (Store-and-Forward) (b) Scenario 2 (Store-and-Forward)

(c) Scenario 1 (CTM) (d) Scenario 2 (CTM)

Figure 10. Norm of uncontrollable output $\| z_{\mathbf{u}} \|_{\mathbf{2}}$.

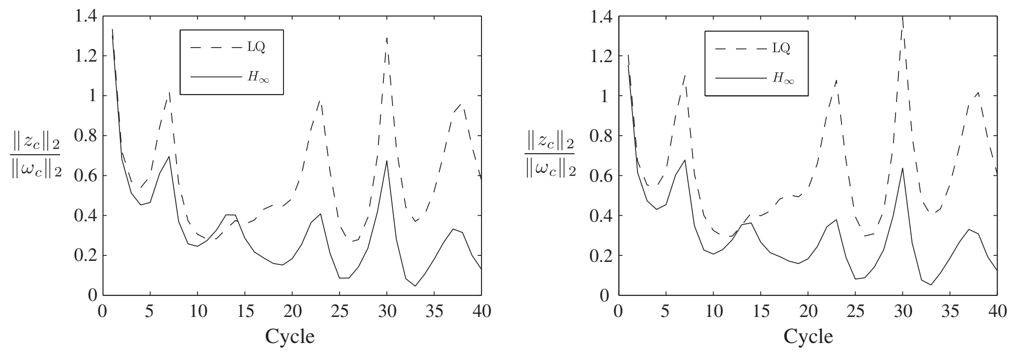

(a) Store-and-Forward (b) CTM

Figure 11. Effect of disturbances $\frac{\|z_c\|_2}{\|\omega_c\|_2}$.

then limits it under 0.8. Indeed, the value of $\frac{\|z_c\|_2}{\|\omega_c\|_2}$ under the H_∞ control is significantly smaller than the one under the LQ approach. Because it has been shown that both methodologies have no influence on the uncontrollable part, the proposed method also leads to better results for the entire system (Figure 12).

We close this section by emphasizing that, because the LQ control strategy must solve a quadratic-programming problem in local intersections at each step [7], our result is more efficient in the sense that the feedback can be directly applied for each step, which gives us a flexibility on the level of its applications.

DOI: 10.1002/atr

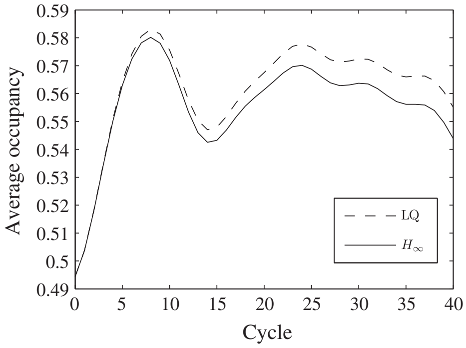

(a) Store-and-Forward

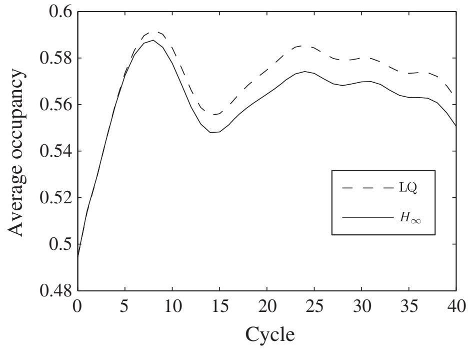

(b) CTM

Figure 12. Average occupancies $\bar{\mathbf{z}}=\frac{\sum \mathbf{z_i}}{\mathbf{n}}$.

6. CONCLUSIONS

In this paper, we proposed a robust controller for the disturbance attenuation of transportation network. The errors between real traffic demands and the nominal ones are considered as disturbances, and a constrained H_∞ control has been formulated in terms of the maximization of the tolerance under control constraints. The necessary and sufficient solution has been presented in Theorem 3. However, such solution needs to solve the non-LMI (64), which is an NP-hard problem. This lack of computational efficiency forced us to choose the matrix $\boldsymbol{Q}=\boldsymbol{I}$ in Corollary 1 such that the inequality can be transformed into a linear form. The counterpart of this would be the loss of the optimal character of the tolerance $\frac{\alpha}{\gamma}$. The obtained solution γ^* is just sub-optimal in the sense that $\gamma^* \geq \gamma^{opt}$ where γ^{opt} is the true optimal solution of Theorem 3. In the simulation study, we compared the constrained H_∞ control method with the LQ one presented in [7]. Two evaluation criteria have been used for the comparison: the total time spent and the relative queue balance. It has been shown that our method leads to significant reductions of both evaluation criteria compared with the LQ approach. The further investigations should deal with the comparison of the proposed constrained H_∞ control with other strategies (e.g., model predictive control) in more elaborated (e.g., microscopic) simulation as well as in real systems.

7. LIST OF SYMBOLS AND ABBREVIATIONS

x_i	the number of vehicles in the lane i
r_i	the flow rate of the traffic demand to the lane i
d_i	the flow rate of the exit flow from the lane i
$\sigma_{i,j}$	the rate of the traffic flow from the lane j to the lane i
T	the discrete-time step
g_i	the effective green time of the lane i in one cycle
c	the cycle time
s_i	the saturation flow rate of the lane i
$\lambda_{i,j} \in [0, 1]$	the turning rate from the lane j to the lane i
$\lambda_{i,i} \in [0, 1]$	the exit rate of the lane i

REFERENCES

1. Robertson DI. TRANSYT method for area traffic control. *Traffic Engineering & Control* 1969; **10**:276–281.
2. Bretherton RD, Hunt P, Robertson D, Royle M. The SCOOT on-line traffic signal optimisation technique. *Traffic Engineering & Control* 1982; **23**(4):190–192.
3. Papageorgiou M, Diakaki C, Dinopoulou V, Kotsialos A, Wang Y. Review of road traffic control strategies. *Proceedings of the IEEE* 2003; **91**(12):2043–2067.
4. Daganzo CF. The cell transmission model, part II: network traffic. *Transportation Research Part B: Methodological* 1995; **29**(2):79–93.

DOI: 10.1002/atr

5. Almasri E, Friedrich B. Online offset optimisation in urban networks based on cell transmission model. ITS Hanover, 2005.
6. Flötteröd G, Rohde J. Operational macroscopic modeling of complex urban road intersections. *Transportation Research Part B: Methodological* 2011; **45**(6):903–922.
7. Diakaki C, Papageorgiou M, Aboudolas K. A multivariable regulator approach to traffic-responsive network-wide signal control. *Control Engineering Practice* 2002; **10**(2):183–195.
8. Gazis D, Potts R. The oversaturated intersection. *Proceedings of the Second International Symposium on the Theory of Road Traffic Flow*, London, UK, 1963; 221–237.
9. Aboudolas K, Papageorgiou M, Kosmatopoulos E. Store-and-forward based methods for the signal control problem in large-scale congested urban road networks. *Transportation Research Part C: Emerging Technologies* 2009; **17**(2):163–174.
10. de Oliveira LB, Camponogara E. Multi-agent model predictive control of signaling split in urban traffic networks. *Transportation Research Part C: Emerging Technologies* 2010; **18**(1):120–139.
11. Aboudolas K, Papageorgiou M, Kouvelas A, Kosmatopoulos E. A rolling-horizon quadratic-programming approach to the signal control problem in large-scale congested urban road networks. *Transportation Research Part C: Emerging Technologies* 2010; **18**(5):680–694.
12. Heydecker B. Uncertainty and variability in traffic signal calculations. *Transportation Research Part B: Methodological* 1987; **21**(1):79–85.
13. Ribeiro PCM. Handling traffic fluctuation with fixed-time plans calculated by TRANSYT. *Traffic Engineering & Control* 1994; **35**(6):362–366.
14. Yin Y. Robust optimal traffic signal timing. *Transportation Research Part B: Methodological* 2008; **42**(10):911–924.
15. Zhang L, Yin Y, Lou Y. Robust signal timing for arterials under day-to-day demand variations. *Transportation Research Record: Journal of the Transportation Research Board* 2010; **2192**:156–166.
16. Li J-Q. Discretization modeling, integer programming formulations and dynamic programming algorithms for robust traffic signal timing. *Transportation Research Part C: Emerging Technologies* 2011; **19**(4):708–719.
17. Ukkusuri SV, Ramadurai G, Patil G. A robust transportation signal control problem accounting for traffic dynamics. *Computers & Operations Research* 2010; **37**(5):869–879.
18. Tettamanti T, Varga I, Kulcsar B, Bokor J. Model predictive control in urban traffic network management. *2008 16th Mediterranean Conference on Control and Automation*. Ajaccio, France, 2008; 1538–1543.
19. Tettamanti T, Luspay T, Kulcsar B, Peni T, Varga I. Robust control for urban road traffic networks. *IEEE Transactions on Intelligent Transportation Systems* 2014; **15**(1):385–398.
20. Lin S, De Schutter B, Xi Y, Hellendoorn H. Fast model predictive control for urban road networks via MILP. *IEEE Transactions on Intelligent Transportation Systems* 2011; **12**(3):846–856.
21. Diakaki C. Integrated control of traffic flow in corridor networks. Ph.D. Thesis, Department of Production Engineering and Management, Technical University of Crete, Chania, Greece, 1999.
22. Wakasa Y, Hanaoka K, Iwasa T, Tanaka K. Modeling for control of traffic signal systems. *Proceedings of 2005 IEEE Conference on Control Applications, CCA*, 2005; 1594–1599.
23. Sontag ED. *Mathematical Control Theory: Deterministic Finite Dimensional Systems*. Springer, 1998.
24. Axler S. *Linear Algebra Done Right* (2nd). Springer, 1997.
25. Doyle J, Glover K, Khargonekar P, Francis B. State-space solutions to standard H_2 and H_∞ control problems. *IEEE Transactions on Automatic Control* 1989; **34**(8):831–847.
26. Zhou K, Doyle JC, Glover K. *Robust and Optimal Control*. Prentice-Hall, Inc.: Upper Saddle River, NJ, USA, 1996.
27. Doyle J, Packard A, Zhou K. Review of LFTs, LMIs, and μ. *Proceedings of the 30th IEEE Conference on Decision and Control*, Vol. **2**. Brighton, UK, 1991; 1227–1232.
28. Boyd S, Ghaoui LE, Feron E, Balakrishnan V. *Linear Matrix Inequalities in System and Control Theory*. SIAM: Philadelphia, USA, 1994.
29. Hennet JC. Une extension du lemme de Farkas et son application au problème de régulation linéaire sous contrainte. *Comptes rendus de l'Académie des sciences. Série 1, Mathématique* 1989; **308**(13):415–419.
30. Fu M, Luo Z-Q. Computational complexity of a problem arising in fixed order output feedback design. *Systems & Control Letters* 1997; **30**(5):209–215.
31. Boyd S, Vandenberghe L. *Convex Optimization*. Cambridge University Press: New York, USA, 2004.
32. Grant M, Boyd S. CVX: MATLAB software for disciplined convex programming, version 1.21, Apr. 2011.
33. Chang T-H, Sun G-Y. Modeling and optimization of an oversaturated signalized network. *Transportation Research Part B: Methodological* 2004; **38**(8):687–707.

DOI: 10.1002/atr